**SLOPE REDUCTION OF SMALL POLAR CRATERS ON THE MOON.** Ariel N. Deutsch[1], Lior Rubanenko[2], Jennifer L. Heldmann[1], Anthony Colaprete[1], Richard Elphic[1], Michael K. Barker[3], Caleb I. Fassett[4], James W. Head[5], and Valentin T. Bickel[6], [1]NASA Ames Research Center, Moffett Field, CA 94035 (ariel.deutsch@nasa.gov), [2]Stanford University, Stanford, CA 94305 (liorr@stanford.edu), [3]NASA Goddard Space Flight Center, Greenbelt, MD 20771, [4]NASA Marshall Space Flight Center, Huntsville, AL 35804, [5]Brown University, Providence, RI 02912, [6]Swiss Federal Institute of Technology Zurich, CH.

**Introduction:** Previous works observed a shallowing of lunar polar craters with latitude that may be related to the accumulation of ice [1–3]. If ice accumulations are indeed influencing crater morphometries, their influence on crater slope is expected to be greater on (typically colder) pole-facing (PF) slopes than it is on equator-facing (EF) slopes [2], consistent with concentrations of H-bearing volatiles being biased towards PF slopes at the south pole [4].

We analyzed the slopes of permanently shadowed regions (PSRs) [5] and non-PSRs of PF and EF crater walls at the lunar south pole. We then modeled the distribution of expected slopes for PSR and non-PSR polar craters and compared the results.

As expected, PSR EF slopes are steeper than non-PSR EF slopes (high slopes are more likely to cast a PSR). However, for PF slopes, this trend reverses; PSR PF slopes are shallower than non-PSR PF slopes. This reversed trend may be the signature of volatiles that have preferentially affected PF slopes. Here we discuss potential mechanisms that may cause this PSR shallowing and implications for exploration strategies.

**Observational Analysis:** *Methods.* We identified craters that (i) are located between 80°S and 90°S, (ii) have diameters between 1 and 5 km (to mitigate scale-dependent degradation effects), (iii) are not located on the walls of larger craters (to mitigate effects of impacts into sloped terrain), (iv) are not superposed by craters >~100 m (to mitigate influences of imprinting topography), and (v) are not obvious secondary craters (to mitigate effects of secondary cratering on crater geometry). This resulted in a study population of 564 south polar craters. Analysis of the north pole is ongoing.

For each crater, we extracted slope from 120-mpp Lunar Orbiter Laser Altimeter (LOLA) models [6]. We defined EF slopes by azimuths of 180°E ± 20° and PF slopes by azimuths of 0°E ± 20° [6]. For each crater, we found the 90$^{th}$ percentile slope value for four zones: EF PSR, EF non-PSR, PF PSR, and PF non-PSR. Depending on a crater's geometry and illumination conditions, it may not have all four zones.

*Results for Equator-Facing Walls.* PSR slopes tend to be steeper than non-PSR slopes for EF crater walls (**Fig. 1a**). This result is consistent with what one would expect from the crater's geometry; the presence of steep slopes at the low-illuminated poles gives rise to PSRs, while flatter terrains are not as shadowed.

*Results for Pole-Facing Walls.* The pattern reverses for PF crater walls; PSR slopes tend to be shallower than non-PSR slopes (**Fig. 1b**). Curiously, this is opposite from what one would expect based on the crater's geometry.

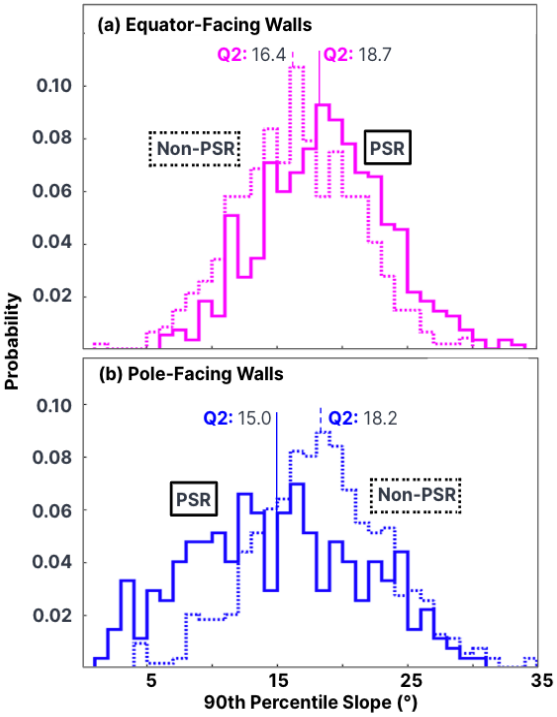


**Figure 1.** *Histograms show the 90th percentile slope for PSRs (solid line) and non-PSRs (dashed line) of* ***(a)*** *equator-facing and* ***(b)*** *pole-facing walls. Q2 = histogram median.*

**Modeling Analysis:** *Methods.* The height of a shadow cast by a parabolic crater with a depth/diameter (d/D) ratio Δ can be calculated as the difference between the shadow plane and the topographic relief of the crater. For a one-dimensional cross section passing through the crater center, the height of the shadow ($h_s$) is,

$$\frac{h_s(f)}{d} = f\left[\frac{\cot z}{\Delta} - 4(1-f)\right] \qquad (\boldsymbol{Eq.\ 1})$$

where $z$ is the solar zenith angle and $f \equiv x/D$, where x is the horizontal distance from the crater rim. For craters whose sizes are much smaller than the radius of the

Moon, neglecting the Moon's obliquity changes, the solar zenith angle at noon is equal to the local latitude: $z = \varphi$. Since at noon the crater also casts the shallowest possible instantaneous shadow, ***Eq. 1*** also defines the maximum height of the shadow within the crater as the Sun sweeps across the sky, and, as a result, the maximum potential ice infill (**Fig. 2a**).

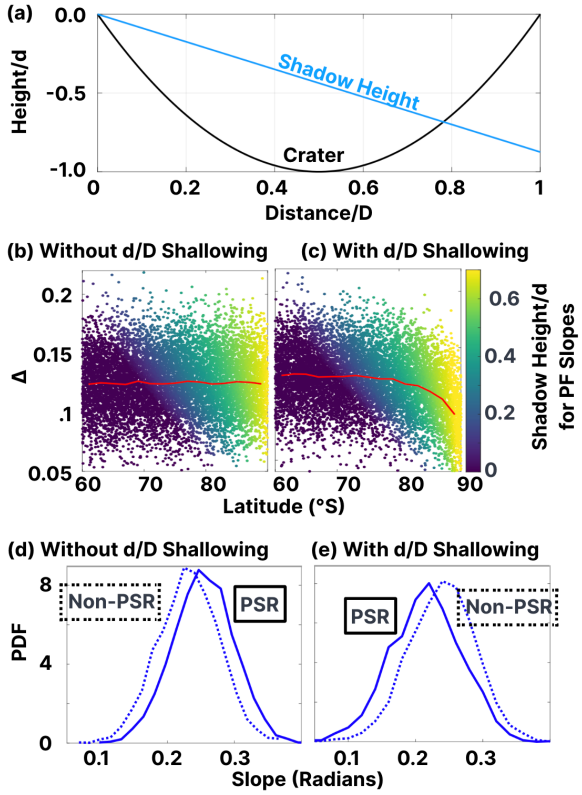


**Figure 2.** ***(a)*** *Modeled crater topography ($\Delta = 0.2$) and height of a shadow cast at noon, $\varphi = 85°$.* ***(b,c)*** *Monte-Carlo simulations (N=10,000) of craters with and without polar shallowing trend as in [2].* ***(d,e)*** *Probability density functions of PF slopes with and without shallowing trend.*

Since the height of the PSR naturally increases with $\varphi$ and $\Delta$, high-latitude steep slopes are more likely to cast a permanent shadow than shallow slopes. To demonstrate this effect, we assumed d/D is normally distributed $\Delta \sim N\ (\mu_\Delta = 0.125,\ \sigma = 0.025)$ [2] and plotted the shadow height at the center of the PF slope ($f = 1/4$) for $\mu_\Delta$ that is constant with latitude (**Fig. 2b**) and $\mu_\Delta$ that decreases with latitude by up to 10%, as in [2] (**Fig. 2c**). Then, we plotted histograms of craters' PF slopes for $h_s/d = 0.1$ (**Figs. 2d,e**).

*Results.* Our Monte Carlo model shows that when the mean d/D does not change with latitude (**Fig. 2b**), high-latitude PF steep slopes are more likely than PF shallow slopes to cast high shadows. However, when polar craters are modeled with a shallowing trend as in [2] (**Fig. 2c**), this trend reverses; the likelihood that a shallow crater will cast a PSR increases (PSR density function moves to the left). In this case, the height of the shadow is a more sensitive function of the noon incidence angle than of the crater's d/D.

**Discussion and Conclusions:** Our finding that the PF slopes of polar craters as measured from LOLA are more likely to be shallow if they are in PSR supports the findings of [1–3] that a polar shallowing trend is present for craters 1–5 km near the south pole of the Moon. Our second finding, that this trend only occurs for PF slopes but not for EF slopes, is consistent with the hypothesis that this slope reduction is related to volatiles.

One possibility is that volatile have accumulated preferentially of PF slope, leading to slope reduction. Analysis of the volume of volatiles required to match the observed slope reduction is ongoing, but reduced d/D suggest this could be several tens-hundreds of meters of volatiles [1–3].

Alternatively, the reduction of polar slopes could be caused by volatile-related slope failures. For example, PF slopes on Mars have been shown to be systematically gentler than EF slopes in particular latitudinal belts where ground ice is expected [7]. At these locations, creep (no melting) and/or freeze-thaw cycles may be responsible for the downslope movement of ice, leading to slope reduction of ice-bearing craters [7].

Crater slopes can be influenced by a myriad of factors, including the crater-forming conditions (e.g., impact angle, target composition, target slope) as well as modification processes (e.g., regolith gardening, impact bombardment and emplacement of distal ejecta, thermal cycling) and the crater's age (i.e., exposure time to modification processes). Here we used population statistics of >500 similarly sized and similarly located craters to provide insight into the possible presence of volatiles on the Moon.

Initial results suggest that volatiles may be preferentially cold-trapped beneath PF permanently shadowed slopes at the lunar south pole. These volatiles appear to be present at such an abundance that they have reduced the slopes of their host craters. Work is ongoing to quantify this abundance. These results can help provide exploration strategies for targeting ice-rich areas during upcoming lunar missions [e.g., 8], including the Artemis Campaign.

**References:** [1] Kokhanov A. A. et al. (2015) *SSR, 49,* 295–302. [2] Rubanenko L. et al. (2019) *Nat Geo, 12,* 597–601. [3] Figuera R. M. et al. (2022) *Rem Sens, 14,* 450. [4] McClanahan T. P. et al. (2015) *Icarus, 255,* 89–99. [5] Mazarico E. et al. (2011) *Icarus,* 211, 1066–1081. [6] http://imbrium.mit.edu/ [7] Kreslavsky M. A. and Head J. W. (2003) *GRL, 30,* GL017795. [8] Colaprete A. et al. (2020) *LPS LI,* #2241.